Available online at www.eccomasproceedia.org
Eccomas Proceedia SMART (2023) 679-690

ECCOMAS
Proceedia

X ECCOMAS Thematic Conference on Smart Structures and Materials
SMART 2023
D.A. Saravanos, A. Benjeddou, N. Chrysochoidis and T. Theodosiou (Eds)

SHAPE CONTROL OF ADAPTIVE FUNICULAR STRUCTURES

Guerra Riaño, Andrés F.*AND Várkonyi, Péter L.†

*Dept. of Mechanics, Materials, and Structures
Budapest University of Technology and Economics
Budapest, Hungary
e-mail: guerra.andres@edu.bme.hu

† Dept. of Mechanics, Materials, and Structures
Budapest University of Technology and Economics
Budapest, Hungary
e-mail: varkonyi.peter@epk.bme.hu

Abstract. Funicular structures transfer their loads through axial forces. This feature makes them more efficient than structures subject to shear and bending, but in turn, the loads determine the structural shape and vice versa. Nevertheless, structures are often subjected to loads varying in time and funicularity requires adaptation of shape. Flexible tensile structures e.g. cables and textiles adapt their forms to loads spontaneously. In contrast, the bending stiffness of compression structures does not allow spontaneous change of shape, thus more structural material is needed to prevent bending-induced mechanical failure. At the same time pure compression or mixed structures offer better solutions in some structural applications

The purpose of this study is to use sensory feedback about a structure's deformations to guide the structure to a funicular shape which is time-dependent and unknown to the controller. We consider a discrete model of a cantilever structure composed of rigid bars and elastic joints equipped with sensors measuring bending moments and rotary actuators. We aim to guide the structure towards different funicular configurations when the external load is unpredictable and not directly observable. The efficiency of the system under different control policies is studied with emphasis on stability under constant load and ability of the controller to react to rapidly changing loads.

Key words: Funicular structures, adaptive structures, shape control

1 INTRODUCTION

The aim of adaptive architecture is to use elements changing morphology in response to environmental conditions. As inspiration, nature provides adaptive structures composed of hygroscopic materials which respond to change of moisture and temperature changes. This idea inspired the development of smart materials used in facades [1] to collect rainwater and performthermal control [2].

Peer-review under responsibility of the organizing committee of SMART 2023.
doi: 10.7712/150123.9822.444919

Adaptation guided by feedback control has been applied extensively in structural dynamics to reduce the effect of dynamic loads produced by wind [3], and earthquakes [4] [5]. Adaptive response to quasi-static loads has gained less attention in the research community. However, some recent works aim to develop adaptive planar reticular structures [6] and spatial structures [7] under varying loads in order to reduce load-induce deformations, and to minimize whole-life energy.

The design process of funicular structures is an important example of shape adaptation to static loads. These structures transfer loads through pure axial or in plane forces. Funicular structures are often much stronger and more efficient than those, which are subject to shear and bending. Examples of these structures include arches, cables, tensegrities, among others. An important feature is that the external loads determine the shape of the structure and vice versa [8]. Nevertheless, optimal forms are not known in advance and consequently form findingmethods are required in the design process [9].

A particularly challenging situation occurs if a funicular structure is subjected to time-dependent loads. Funicular structures can be classified as form- active or passive systems. Flexible tension structures such as cables, and membranes deform in such a way that their force trajectory coincides with the structural shape. Consequently, the shape self-adapts spontaneously to varying load. Nevertheless, in the case of form-passive systems like pure compression structures with high flexural stiffness, form cannot self-adjust under load variation. Thus, varying loads create undesirable bending moments. Importantly, flexural stiffness is crucial to these structures, as structures with high compliance may suffer from various forms of elastic instability such as buckling.

Commonly, structures are designed to resist the worst loading scenario, nevertheless during most of their lifetime they are under more favorable load conditions. This design rule results in the addition of structural material unused during most of the time and restrictions in architectural design [10]. Feedback control and shape adaptation can significantly reduce excess material.

Shape adaptation of funicular compression or tension-compression structures reacting to different load cases without loss funicularity has a strong potential due to the high sensitivity of such structures to load distribution. We believe that adaptive funicular structures provide an important new category of light-weight structures, which inherit the robust funicularity of cable structures, but have a wider range of application.

Finite degree-of-freedom models of structures give rise to a set of ordinary differentials equations as the equations of motion. Control policies often follow classical ideas such as PID (proportional-integral-derivative) control. Controller parameters can be set by engineering tuning rules or by dynamic analysis [3] taking into account the requirements of stability, robustness, and sufficiently low response time [11]. Various types of actuators can be used to transform the output of a control unit into element action to change geometries [12]. In architectural scale, themost common types are hydraulic, electric and pneumatic actuators. The present work focuseson optimal control policy through the example of actuated rotary joints of a funicular cantileverstructure. We extend ideas published in a previous paper [13] by using a more realistic controlpolicy and by equipping the system with internal damping to improve

stability and response time.

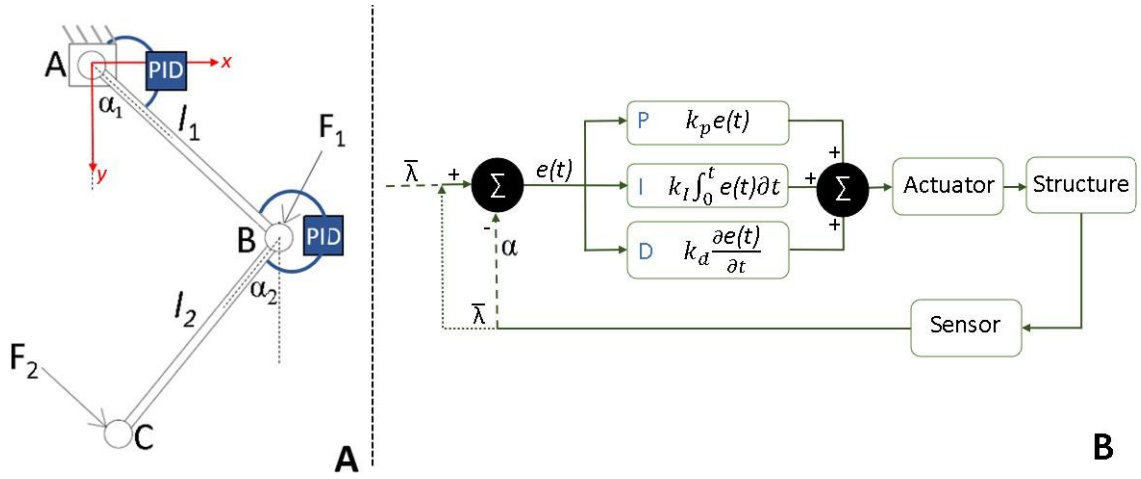

Figure 1: A: Mechanical model of a two-link adaptive cantilever. B: Schematic representation of a closed loop PID controller. Black circles represent summation, and $e(t)$ is an error function. Dashed lines refer to the position control discussed in Section 3, dotted lines refer to funicular control (Section 4). Continuous lines refer to both cases.

2 A TWO-LINK CANTILEVER STRUCTURE

A simple two dimensional, two-degree-of-freedom model of a cantilever structure is showed in Figure 1A. It is composed of two rigid, massless bars with lengths l_1, l_2 and two point masses m_1, m_2 at points B and C. The bars are connected to the environment at node A, and to each other at point B by pin joints. External force loads F_i are applied at B and C. The shape of the bar is characterized by the angles α_1, α_2 and the pin joints are actuated by torques τ_1 and τ_2.

In order to analyze the dynamics of this structure, the equations of motion are formulated using Euler-Lagrange equations. Position coordinates (r_{1x}, r_{1y}) of node B, and coordinates (r_{2x}, r_{2y}) of C in a coordinate system centered at A can be written as

$$_x = l \sin\alpha \ , r_y = -l \cos\alpha \ , \quad (1)$$

$$_{2x} = l \sin\alpha + l_2 \sin\alpha_2 \ , \ r_{2y} = -l \cos\alpha - l_2 \cos\alpha_2. \quad (2)$$

The kinetic energy of the system is

$$T = \frac{1}{2} m \ v^2 + \frac{1}{2} m_2 v_2^2, \quad (3)$$

where

$$v_i^2 = \dot{}_{ix}(t)^2 + \dot{}_{iy}(t)^2. \quad (4)$$

Let the coordinates of force vector F_i be denoted by (F_{ix}, F_{iy}). The potential energy associated with the external forces is given by

$$V = -F_{1y} l_1 \cos\alpha_1 - F_{2y}(l_1 \cos\alpha_1 + l_2 \cos\alpha_2) - \ldots \\ \ldots F_{1x} l_1 \sin\alpha_1 - F_{2x}(l_1 \sin\alpha_1 + l_2 \sin\alpha_2). \quad (5)$$

Then, the Lagrangian $L = T - V$ is given by

$$L = \\ \frac{1}{2} m_1 v_1^2 + \frac{1}{2} m_2 v_2^2 - \\ \left[-F_{1y} l_1 \cos\alpha_1 - F_{2y}(l_1 \cos\alpha_1 + l_2 \cos\alpha_2) - F_{1x} l_1 \sin\alpha_1 - F_{2x}(l_1 \sin\alpha_1 + l_2 \sin\alpha_2)\right] \quad (6)$$

We use Euler-Lagrange equation for α_i:

$$\frac{d}{dt}\left(\frac{d}{\frac{d}{dt}\alpha_i} L\right) = \frac{d}{d\alpha_i} L + g_i \quad (7)$$

where g_i are generalized forces depending on the actuator torques τ_i as:

$$g_1 = (\tau_1 - \tau_2),\ g_2 = \tau_2.$$

From equation (7) a system of linear equations $\mathbf{Ax} = \mathbf{b}$ is obtained:

$$\boldsymbol{A} = \begin{bmatrix} l_1^2 m_1 + l_1^2 m_2 & l_1 l_2 m_2 \cos(\alpha_1 - \alpha_2) \\ l_1 l_2 m_2 \cos(\alpha_1 - \alpha_2) & l_2^2 m_2 \end{bmatrix} \quad (8)$$

$$\boldsymbol{x} = [\ddot{\alpha}_1(t), \ddot{\alpha}_2(t)]^T \quad (9)$$

$$\boldsymbol{b} = [b_1, b_2]^T \quad (10)$$

$$b_1 = -l_1 l_2 m_2 \sin(\alpha_1 - \alpha_2)\, \dot{\alpha_2}^2 + F_{1x}\, l_1 \cos\alpha_1 + \cdots \\ \ldots F_{2x}\, l_1 \cos\alpha_1 - F_{1y} l_1 \sin\alpha_1 - F_{2y} l_1 \sin\alpha_1 - \tau_1 + \tau_2 \quad (11)$$

$$b_2 = l_1 l_2 m_2 \sin(\alpha_1 - \alpha_2)\, \dot{\alpha_2}^2 + F_{2x} l_2 \cos\alpha_2 - F_{2y} l_2 \sin\alpha_2 - \tau_2 \quad (12)$$

where ^{T} means transpose. The angular acceleration can be expressed as $\mathbf{x} = \mathbf{A}^{-1}\mathbf{b}$.

3 A CLASSICAL CONTROL PROBLEM

A classical 'position control' task is to maintain a preferred structural form regardless of the external force. This type of control does not ensure funicularity, nevertheless it is discussed here because of its tight relation to funicular control presented in the next section.

We seek to maintain fixed values $\alpha_1=\lambda_1$, $\alpha_2=\lambda_2$. It is assumed that the state variables α_1, α_2 can be observed directly (state feedback).

We assume that the actuators are driven by PID (proportional-integral-derivative) controllers,as illustrated by dashed and continuous lines in Figure 1B. This type of controller is routinely used in many situations, including theoretical control problems and industrial applications.

Each PID controller delivers control torque

$$\tau_i(t) = \tau_i^p(t) + \tau_i^d(t) + \tau_i^I(t) \tag{13}$$

$$= -k_{pi}(\alpha_i(t) - \lambda_i) - k_{di}\dot{\alpha}_\iota(t) - k_{Ii}\int_0^\tau(\alpha_i(x) - \lambda_i)dx \tag{14}$$

which is the sum of a term τ_i^p proportional to the deviation of the corresponding angle from the prefererred value, a derivative term τ_i^d proportional to the derivative of the deviation, and an integral term τ_i^i proportional to the integral of the same quantity over time. The first term is responsible for driving the angles towards the target values; the second term damps oscillations, in order to avoid dynamic instability, and the last term is responsible for the removal of residual error on long time scales.

It is important to note that the first two terms ($\tau_i^p(t)$ and $\tau_i^d(t)$) of the controller can be implemented as passive elements: namely a linear torsional spring with torque-free angle λ_i, and a linear damper. As we show below, the effect of the integral term is equivalent to an activeelement, varying the torque-free angle of the spring over time.

In order to show this, we consider the PI part of the controller

$$\tau_i^{pi}(t) = \tau_i^p(t) + \tau_i^I(t) = -k_{pi}(\alpha_i(t) - \lambda_i) - k_{Ii}\int_0^t(\alpha_i(x) - \lambda_i)dx \tag{15}$$

which is equivalent to

$$\tau_i^{pi}(t) = -k_{pi}\left(\alpha_i(t) - \overline{\lambda_\iota}(t)\right) \tag{16}$$

$$\overline{\lambda_\iota}(t) = \lambda_i - \frac{k_{Ii}}{k_p}\int_0^t(\alpha_i(x) - \lambda_i)\,dx \tag{17}$$

By taking derivatives of both sides of the last equation, we obtain

$$\dot{\overline{\lambda_\iota}}(t) = -\frac{k_I}{k_p}(\alpha_i(t) - \lambda_i) \tag{18}$$

i.e. the integral controller of the original system is equivalent to varying the torque-free angle $\bar{\boldsymbol{\lambda}}_i$ of the torsional spring with a rate proportional to the deviation of that angle from the preferred value λ_i.

Before proceeding with the analysis, we rewrite the equations of motion as a set of first-order differential equations in the state vector composed of angles, angular velocities, and torque-free angles:

$$\dot{y} = f(y) \tag{19}$$

$$y = \left[\alpha\ , \alpha_2, \omega\ , \omega_2, \overline{\lambda}\ , \overline{\lambda_2}\right]^T \tag{20}$$

$$f(y) = \left[\omega_1, \omega_2, \boldsymbol{b}^T\boldsymbol{A}^{-T}, -\frac{k_I}{k_p}(\alpha\ - \lambda\ ), -\frac{k_I}{k_p}(\alpha_2 - \lambda_2)\right]^T \tag{21}$$

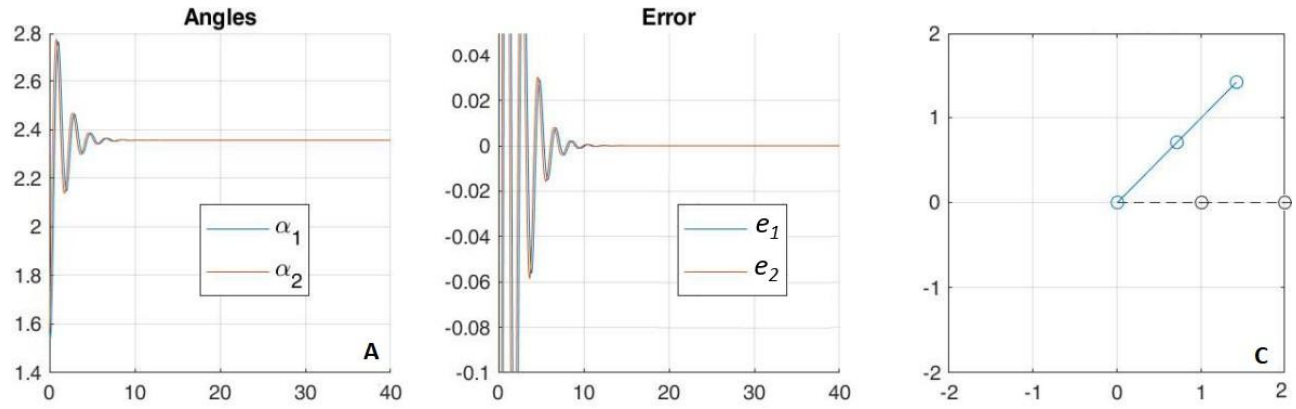

Figure 2: Simulation of the controlled system with a priori chosen target shape. A: time history of joint angles. B: time history of error functions. C: initial and final shapes.

where **A** and **b** were introduced in Section 2.

If an initial condition vector

$$\mathbf{y}_0 = [\alpha_{10}, \alpha_{20}, \dot{\alpha}_{10}, \dot{\alpha}_{20}, \bar{\lambda}_{10}, \bar{\lambda}_{20}]^T \tag{22}$$

is specified, then we obtain an initial value problem for the dynamics of the system, which is amenable to numerical simulation. Figure 2 shows simulation results with constant load $F_{1x} = -0.5$, $F_{2x} = 0$, $F_{1y} = 1$ and $F_{2y} = 1$, controller parameters $k_{p1} = k_{p2} = 50$, $k_{d1} = k_{d2} = 10$ and $k_{I1} = k_{I2} = -1$, and target state

$$\lambda_1 = \lambda_2 = 3\pi/4. \tag{23}$$

Panel A depicts the evolution of angles α_i from initial condition

$$\mathbf{y}_0 = [\pi/2, \pi/2, 0, 0, \pi/2, 0]^T. \tag{24}$$

As we can see in panel B, the error functions

$$e_i(t) = \alpha_i(t) - \lambda_i \tag{25}$$

converge to zero, which indicates stability of the system. Panel C shows initial and final shapes. It should be pointed out that the target shape is not funicular, i.e. the torques in the actuators do not vanish.

4 FUNICULAR SHAPE CONTROL

Our ultimate goal is to control the shape of the structure in such a way that it becomes funicular under unknown external loads. Hence, the desired shape is unknown.

Let F_i and ϕ_i denote lengths and angles of the external forces; F_{1+2} and ϕ_{1+2} are length and angle of the vector sum of the two forces. A funicular shape is charaterized by $\alpha_2 = \phi_2 \mod \pi$,

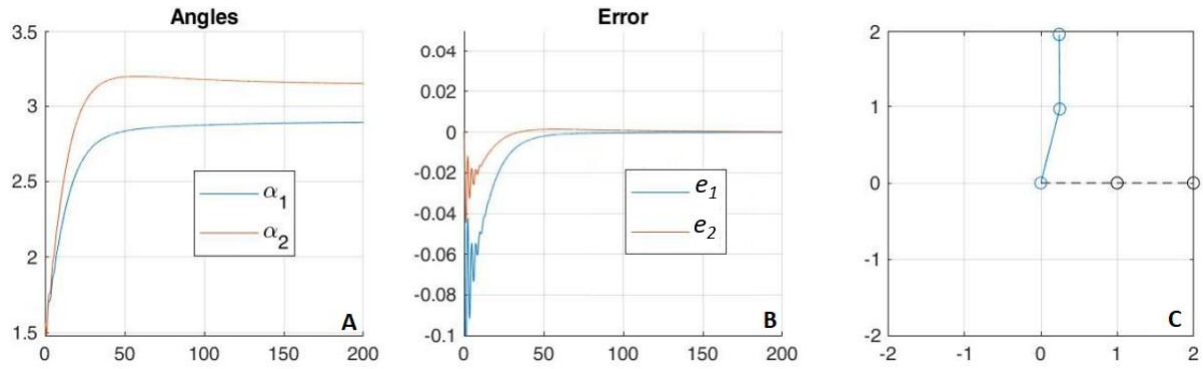

Figure 3: Simulation of funicular shape adaptation

$\alpha_1 = \phi_{1+2} \bmod \pi$. In particular, a funicular shape under pure compression corresponds to $\alpha_2 = \phi_2 + \pi \bmod 2\pi$, $\alpha_1 = \phi_{1+2} + \pi \bmod 2\pi$. The goal of the controller is to restore these unknown values of the angles.

In a static state of the system, the forces and torques acting upon the bars are in equilibrium and the damper is inactive, yielding

$$\tau_2^{pi}(t) = F_2 \sin(\phi_2 - \alpha_2), \tag{26}$$

$$\tau_1^{pi}(t) = F_{1+2} \sin(\phi_{1+2} - \alpha_{1+2}). \tag{27}$$

Consequently, $\tau_i^{pi} = 0$ if and only if the shape of the structure is funicular. Thus, τ_i^{pi} can be used as error function by the controller instead of (25). This observation can be used to modify the previously introduced PID controller in such a way that the torque-free angle is varied according to

$$\dot{\lambda}_i(t) = -\frac{k_I}{k_p}\tau_i^{pi}(t) \tag{28}$$

$$= -K_I\left(\alpha_i(t) - \overline{\lambda_i}(t)\right) \tag{29}$$

The overall scheme of the closed-loop PID controller is also modified, see dotted lines in Figure 1B.

Using the same loads and control gains as in Section 3, but looking for compression-only funicular shape, we repeat the simulation with initial conditions

$$\mathbf{y}_0 = [\pi/2, \pi/2, 0, 0, \pi/2, 0]^T. \tag{30}$$

Figure 3 shows the results of the simulation. Panel C represents the change of shape from initial condition to the expected funicular shape.

Further simulations also uncovered that prescribing positive values of k_{Ii} the system is guided towards tension-only shape, in contrast negative k_{Ii} drives the system to compression-only shape. If the two gain parameters have opposite signs, it is also possible to guide the structure to a mixed compression-tension configuration. (Figure 4).

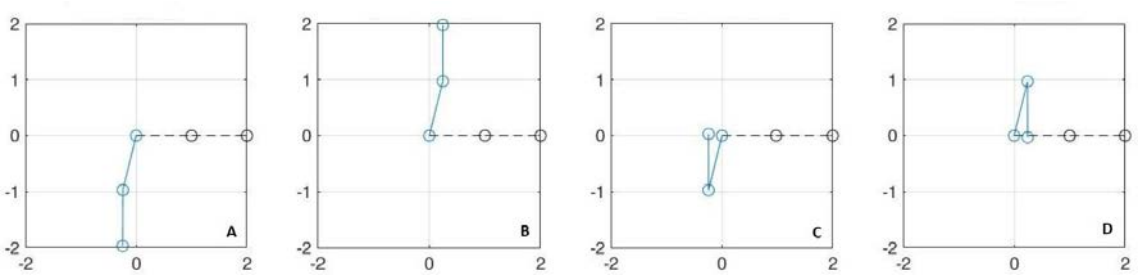

Figure 4: Four funicular shapes found by the closed-loop controller for $F_{1x} = 0.5$, $F_{2x} = 0$, $F_{1y} = 1$, $F_{2y} = 1$, and control parameters $k_{p1} = k_{p2} = 50$ and $k_{d1} = k_{d2} = 10$. The integral gains are $k_{I1} = k_{I2} = 1$ delivering tension-only structure (A), $k_{I1} = k_{I2} = -1$ yielding a pure compression shape (B), $k_{I1} = 1$ $k_{I2} = -1$ (C), and $k_{I1} = -1$ $k_{I2} = 1$ (D). The last two combinations result in mixed tension-compression shapes.

5 TUNING THE CONTROL PARAMETERS

Proper choice of control parameters is essential to guarantee stability, to reduce undesired oscillations and to achieve funicularity in a proper time. In this section we will focus on linear stability analysis.

Linearization of (19) at a the funicular state $\mathbf{y}_F$ yields

$$\dot{\boldsymbol{y}} = f(y) = f(y_F) + \boldsymbol{J}_F(y_F)(y - y_F) + \text{higher order terms}, \tag{31}$$

where $\boldsymbol{J}_F$ is the Jacobian of f. The target shape is an equilibrium, i.e. the first term $f(y_F)$ is zero, and higher-order terms are neglected.

Considering the Jacobian matrix $\boldsymbol{J}_F(y_F)$, the system is stable if and only if all real part of its eigenvalues have negative values. In this case the matrix contains the control gains k_{di}, k_{pi} and k_{Ii} as parameters.

To exemplify this stability analysis, we analyzed the system under vertical loads $F_{1y} = F_{2y} = 1$ and zero horizontal loads, for which the compression-only funicular shape is given by

$$\mathbf{y}_F = [\pi, \pi, 0, 0, \pi, 0]^T. \tag{32}$$

The Jacobian was expressed in closed form, and its eigenvalues were determined numerically. The results of the linear stability analysis are illustrated by contour curves in Figure 5 where the two controllers are assumed to be identical in order to reduce the number of parameters. Two fixed values of the integral gain are considered, and the proportional and derivative terms are varied systematically.

In order to verify the stability analysis, numerical simulations were also carried out with initial conditions

$$\mathbf{y}_0 = [\pi/6, \pi/6, 0, 0, \pi/6, 0]^T, \tag{33}$$

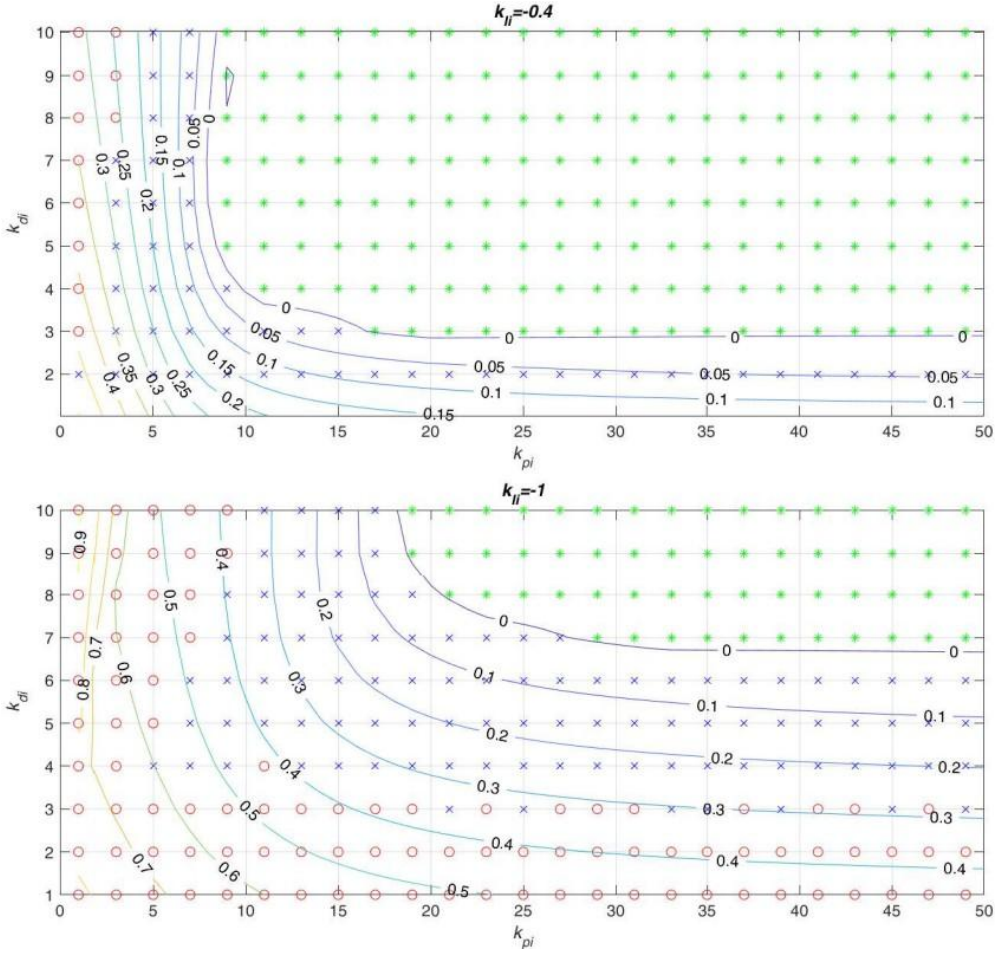

Figure 5: Stability charts of funicular control for 2 values of the integral gain. Contour lines denote real part of the highest eigenvalue, and markers indicate results of numerical simulation

as illustrated by markers in the figure. The result of the simulation was classified as stable (green stars) if the structure arrived to the funicular shape (up to some small numerical tolerance) before the termination of the simulation at time $t_{max} = 1000$. The system was classified as unstable (red circles) if the kinetic energy exceed a certain large threshold value during the simulation. Finally, the simulation was classified as probably unstable (blue x) if none of the previous two events happened during the time of the simulation.

As we can see, the numerical results indicate convergence to the funicular shape exactly when it possesses linear stability. This result suggests that linearly stable equilibria have large basins of attractions, and possibly even global attractivity. More simulation with different initial conditions could provide more solid evidence about the degree of robustness of the equilibria.

It is notable that the system is always unstable below a threshold value of k_{pi}. This is explained by loss of stability due to the classical Euler buckling phenomenon for which the critical

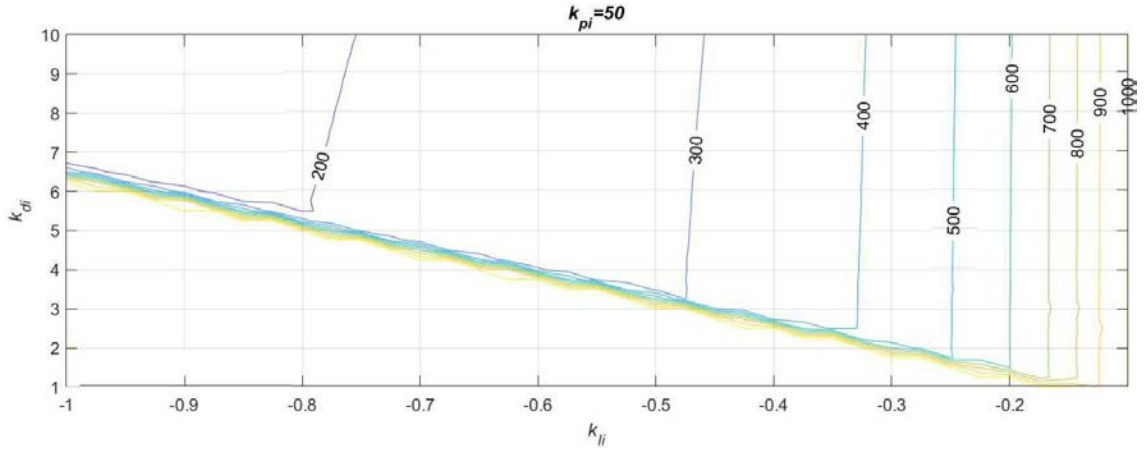

Figure 6: Contour plot of convergence time to funicular shape for $k_{pi} = 50$ for a maximum simulation time t=1000.

value of spring constant is $k_{pi} = 3$. It is also clear that low values of k_{di} also cause instability due to insufficient damping. If larger integral gains k_{Ii} are chosen, then both of the previous two stability threshold increase.

In turn, a high integral term also has an important advantage as it speeds up the response of the system to time-dependent load. Figure 6 summarizes the result of many numerical simulations. In each case, $k_{pi} = 50$ and the other two controller parameters are varied systematically. In each case, the simulation is started with the initial condition given by (33), and the simulation is stopped if the structure converges to funicular shape with a small tolerance, namely, if the cumulative error function

$$e = |(\alpha_2 - \alpha_1 - \lambda_2)| + |(\alpha_1 - \lambda_1)| + |\dot{\alpha}_1| + |\dot{\alpha}_2| \tag{34}$$

drops below 0.001. We can see that by increasing the magnitude of I_{Ii}, the system arrives to the funicular shape faster. At the same time, more derivative control is needed to stabilize the system.

6 CONCLUSIONS

A cantilever structure composed by two inextensible bars connected with hinges actuated by PID controllers. We first studied a classical control problem in which the aim of the controller is to take the structure towards a preferred shape using feedback control. Next, funicular shape control was achieved with a modified error function. By properly choosing the sign of the integral gain, we were able to reach different funicular shapes. The stability and robustness of the controller was studied by combining linear stability analysis with numerical simulation. It was demonstrated that the response time of the controller can be set by proper choice of integral gain, and the stability of the controller is ensured by sufficiently high values of the other two terms. We believe that the ideas demonstrated in this work will be applicable to more complex

and realistic tasks of funicular control, and that adaptive funicular structures deserve further examination in the future.

REFERENCES

[1] S. Di Salvo, *Adaptive Materials Research for Architecture*. Trans Tech Publications Ltd, 2018.

[2] C. Eisenbarth, W. Haase, L. Blandini, and W. Sobek, *Climate-adaptive façades: An integral approach for urban rainwater and temperature management*, 07 2022, pp. 739–746.

[3] J. Rodellar, *Control Theory Sources in Active Control of Civil Engineering Structures*. Dordrecht: Springer Netherlands, 1999, pp. 285–294. [Online]. Available: https://doi.org/10.1007/978-94-011-4611-1_32

[4] R. Guclu, "Sliding mode and PID control of a structural system against earthquake," *Mathematical and Computer Modelling*, vol. 44, no. 1-2, pp. 210–217, 2006.

[5] A. H. Heidari, S. Etedali, and M. R. Javaheri-Tafti, "A hybrid LQR-PID control design for seismic control of buildings equipped with ATMD," *Frontiers of Structural and Civil Engineering*, vol. 12, pp. 44–57, 2018.

[6] G. Senatore, P. Duffour, P. Winslow, and C. Wise, "Shape control and whole-life energy assessment of an 'infinitely stiff' prototype adaptive structure," *Smart Materials and Structures*, vol. 27, no. 1, p. 015022, 2018.

[7] G. Senatore, *Designing and Prototyping Adaptive Structures—An Energy-Based Approach Beyond Lightweight Design*, 08 2018, pp. 169–189.

[8] D. Veenendaal and P. Block, "An overview and comparison of structural form finding methods for general networks," *International Journal of Solids and Structures*, vol. 49, no. 26, pp. 3741–3753, 2012. [Online]. Available: https://www.sciencedirect.com/science/article/pii/S002076831200337X

[9] S. Adriaenssens, P. Block, D. Veenendaal, and C. Williams, *Shell structures for architecture: form finding and optimization*. Routledge, 2014.

[10] G. Senatore, *Robotic Building*. *Designing and Prototyping Adaptive Structures—An Energy-Based Approach Beyond Lightweight Design*. Cham: Springer International Publishing, 2018, pp. 169– 189. https://doi.org/10.1007/978-3-319-70866-9_8

[11] I. Rusnak and L. Peled-Eitan, "Architecture and structure of robust PID controllers," *IFAC Proceedings Volumes*, vol. 47, no. 3, pp. 9289–9294, 2014.

[12] H. Schnädelbach, "Adaptive architecture - a conceptual framework," *in MediaCity* 01 2010.

[13] P. Varkonyi and A. Guerra, “From swinging cables to adaptive funicular structures in architecture,” *IEEE 20th Jubilee International Symposium on Intelligent Systems and Informatics (SISY)* pp. 169–174, 09 2022. doi.10.1109/SISY56759.2022.10036184